

Article

Muon Radiography Investigations in Boreholes with a Newly Designed Cylindrical Detector

Mariaelena D'Errico ^{1,*}, Fabio Ambrosino ^{1,2}, Luigi Cimmino ^{1,2} , Vincenzo Masone ¹, Marco Mirra ¹, Giulio Saracino ^{1,2} and Lorenzo Roscilli ¹

¹ INFN—Sezione di Napoli, Complesso Universitario Monte S. Angelo, 80126 Napoli, Italy

² Physics Department “Ettore Pancini”, Università Degli Studi di Napoli Federico II, 80131 Naples, Italy

* Correspondence: mederrico@na.infn.it

Abstract: Muons are constantly produced in cosmic-rays and reach the Earth surface with a flux of about 160 particles per second per square meter. The abundance of muons with respect to other cosmic particles and their capability to cross dense materials with low absorption rate allow them to be exploited for large scale geological or human-made object imaging. *Muon radiography* is based on similar principles as X-ray radiography, measuring the surviving rate of muons escaping the target and relating it to the mass distribution inside the object. In the course of decades, after the first application in 1955, the methodology has been applied in several different fields. Muography allows us to measure the internal density distribution of the investigated object, or to simply highlight the presence of void regions by observing any excess of muons. Most of these applications require the detector to be installed below the rock being probed. In case that possible installation sites are not easily accessible by people, common instrumentation cannot be installed. A novel borehole cylindrical detector for muon radiography has been recently developed to deal with these conditions. It has been realized with a cylindrical geometry to fit typical borehole dimensions. Its design maximizes the geometrical acceptance, minimizing the dead spaces by the use of arc-shaped scintillators. The details of the construction and preliminary results of the first usage are described in this paper.



Citation: D'Errico, M.; Ambrosino, F.; Cimmino, L.; Masone, V.; Mirra, M.; Saracino, G.; Roscilli, L. Muon Radiography Investigations in Boreholes with a Newly Designed Cylindrical Detector. *Instruments* **2023**, *7*, 2. <https://doi.org/10.3390/instruments7010002>

Academic Editors: Pasquale Arpaia and Martin Pohl

Received: 15 October 2022
Revised: 11 November 2022
Accepted: 17 December 2022
Published: 27 December 2022



Copyright: © 2022 by the authors. Licensee MDPI, Basel, Switzerland. This article is an open access article distributed under the terms and conditions of the Creative Commons Attribution (CC BY) license (<https://creativecommons.org/licenses/by/4.0/>).

Keywords: muography; borehole detectors; cosmic rays

1. Introduction

Muon radiography is developing rapidly and it is increasingly in demand in several new fields. The capability to identify underground cavities, while preserving them from any invasive intervention, makes muography of great interest for archaeology [1,2], mining, and urban applications. Considering the topology of a certain structure under study, and assuming that it is entirely composed of rock, muons spot out the possible presence of cavities, being less absorbed than expected. Traversing a cavity, muons pass through a less dense region, decreasing the number of interactions they undergo. This effect manifests in a local excess of particles, coming from directions within a certain range of angles. This excess is enhanced in a muographic image, where the observed flux is represented relative to the expectations.

The detection of cavities inside heritage buildings can, for instance, prevent possible damages, or can lead to the discovery of unknown cavities, as in the case of pyramids [3]. Furthermore, muon radiography can help in urban security surveys and can be also used as an online monitor of the target of the muographic inspection to discover possible modification, when the thickness range is under ~100 m.

One of the primary difficulties of applying muon radiography for this kind of applications is that often the target is underground and, since the experimental set-up must be installed under the region to be investigated, a suitable underground location to install the apparatus is needed and also must be easily accessible by people. In many cases

this necessity becomes a strong limitation with standard detectors. We developed a new compact borehole detector to deal with this issue. Furthermore, the usage of boreholes allows us to investigate deeper in the underground, up to the kilometer scale, where, for instance, gas reservoirs, salt domes, geological anomalies can be found.

The novel detector has a cylindrical geometry, and its size can fit standard realizable drilled wells. In the following, the detector is described in exact detail, and the results of the test phase and preliminary underground applications are presented.

2. The Detector

The new borehole detector has a cylindrical sensitive surface, realized through the use of scintillators in the shape of arcs. This geometry allows the acceptance to be maximized with respect to the compact size. It is 1 m long and has a 24 cm diameter. The sensitive elements are scintillators in the shape of arcs covered by a layer of scintillator bars parallel to the cylinder axis.

The cylindrical detector consists of 64 inner layers of arc-shaped scintillators and one outer layer of 1 m bars arranged axially. It is divided in two semi-cylindrical sections, each covering 166 horizontal degrees. Between the two sections, two 14 degrees empty gaps are interposed, necessary to leave space for devices reading arcs. These gaps are the major inefficiency source of the detector, even though they don't determine any completely dead zone, but lower the efficiency of the corresponding angular regions. Thus, the detector is oriented in the way that these gaps correspond to regions not included in the desired field of view. Considering a system of cylindrical coordinates the bars are meant to measure the hit angle ϕ , while the arcs provide the z coordinate, as shown in Figure 1. The bars have a rectangular section of 8.5 mm \times 6.5 mm. Arcs have internal and external radius of 83 and 93 mm respectively and the height is 15 mm. Each semi-cylinder is composed of 64 layers of arc pairs, for a total of 128 arcs covered by 32 bars. The whole detector thus consists of 256 arcs and 64 bars optically coupled with Silicon Photomultipliers (SiPMs). Since bars are read from both sides, the apparatus includes a total of 384 photosensors. If positioned vertically, the detector provides an average angular resolutions of the muon direction of about 0.7° and 3° in azimuth and zenith respectively.

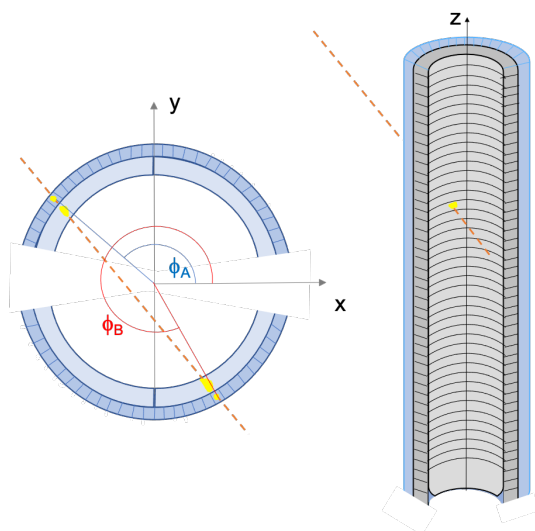


Figure 1. Scheme of the geometry and disposition of the sensitive elements that provide the cylindrical coordinates of the muon impact point.

Scintillators are hosted in containers realized in Acrylonitrile Butadiene Styrene (ABS) with a 3D printer; each container consists of 16 layers of holes to insert arcs and 32 vertical holes to insert bars. Each semicylinder is obtained by stacking 4 containers.

The SiPMs used are S13360-3050PE by Hamamatsu and have a sensitive area of $3 \times 3 \text{ mm}^2$. The sensors are read by a dedicated Front-End and DAQ electronics, based on the experience with previous muon radiography projects [4]. The system has been developed in response of the peculiar necessities of muon radiography experiments, paying particular attention to the compactness and power consumption. Indeed, FEE boards must be compact enough to be housed in the small space inside the cylinder (Figure 2). The FEE electronics is very low power consuming, about 30 W for the whole detector, since many muon radiography applications need the detector to be installed in places where direct electricity is not available and therefore it is necessary to use alternative sources, such as photovoltaic or wind power. It is also important to avoid producing too much heat, since heat exchange with the outside is limited due to the watertight shell protecting the detector. Each slave board is based on the EASIROC ASIC [5], an easy and versatile readout device specifically developed for SiPMs. A total of 12 boards are embedded in the cylinder body, each connected to 32 SiPMs. A Digital to Analogical Converter (DAC) assigns a programmable voltage threshold to the boards; if this threshold is exceeded by one of the 32 SiPMs, the board produces a fast logic signal (OR32). The produced OR32 are sent to a MASTER board which enables the data acquisition if the programmed trigger logic is satisfied. The MASTER is provided with an FPGA for the data transfer with the FEE and a Raspberry-Pi computer for communicating with the internet. The detector is also equipped with an Arduino to monitor temperature and humidity, measured by four sensors (HDC1050 by Texas Instruments) inside the detector housing.

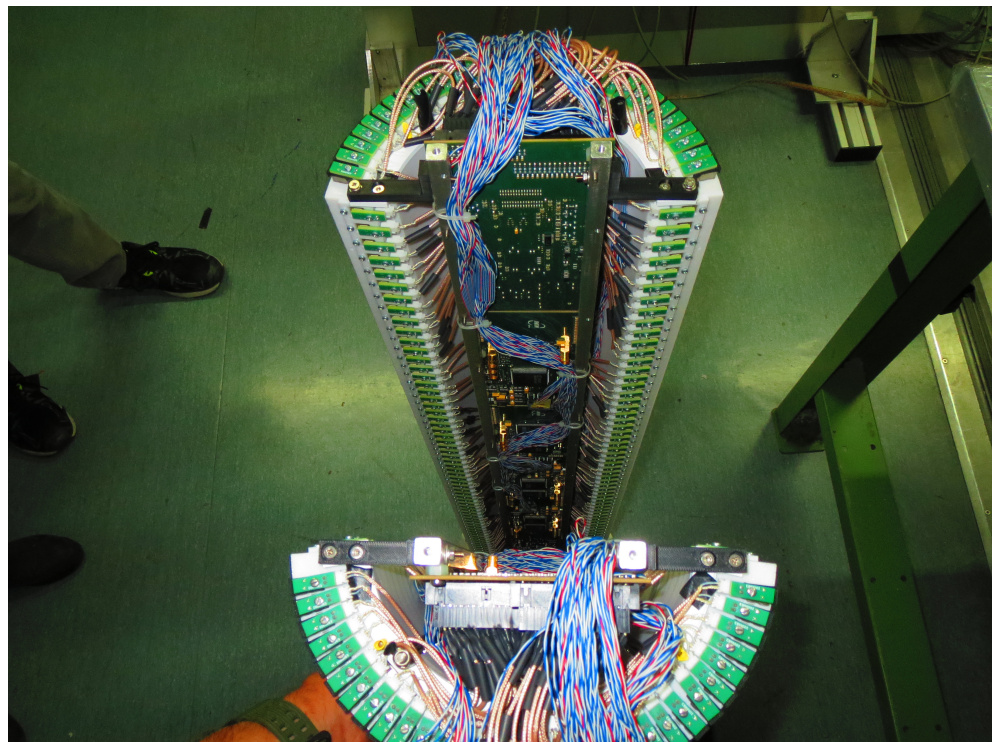


Figure 2. Cylindrical detector opened. Four FEE boards are embedded in each semi-cylinder.

The detector is finally inserted in a stainless steel watertight shell and its final dimensions are 25 cm diameter and 1.2 m length. The final assembly of the detector is shown in Figure 3.



Figure 3. Final assembly of the cylindrical muon detector. On the left, the detector sensitive body before being inserted in the watertight shell (right).

DAQ System

When a muon passes through the detector, the intercepted scintillator elements react by producing light that is translated through the chain SiPM-electronics in over-threshold signals. Signals overcoming the threshold are sent to the Master board, which enable the Data Acquisition (DAQ) after checking if the trigger logic is satisfied.

A FEE board provides a Local Trigger (LT) when at least one of the 32 channels has a signal above the threshold. Threshold values are set in order to avoid dark-noise triggering the boards. The optimal working point of the detector is thus set according to the requirement of negligible dark noise contamination. Since dark noise depends on the temperature, the detector is provided with a system that automatically changes the operating voltage when working conditions change, compensating for fluctuations in the SiPM breakdown voltage.

When a Global Trigger (GT) occurs, the DAQ is activated. The GT logic is programmable; for the present applications the set-up trigger logic can be described as follows. Considering A11, A12, A21 and A22 the OR of the 4 stacks of arcs, and B1, B2 the two groups of bars of each semi cylinder, the GT requires:

$$(B1 \cap (A11 \cup A12)) \cup (B2 \cap (A21 \cup A22)) \quad (1)$$

meaning that at least 1 semi-cylinder must be fired, involving at least one bar and one arc.

3. Free-Sky Data-Taking

Performance of the detector has been tested first on a free-sky exposure. Installing the detector for about a week on the roof of the Physics department of the University of Naples Federico II, far away from any absorbing obstacle, a mean trigger rate (GT logic described in Equation (1)) of about 38.4 Hz and maximum fluctuations within 6.4% have been measured.

The track reconstruction algorithm requires two “signal points” in the same events. A signal point is identified when at least a bar and an arc are hit simultaneously and are geometrically compatible, meaning that if we ideally divide the cylinder in four sections, corresponding to the four stacks of arcs, the bar and arc providing a signal must be part of the same section. Then, when two signal points are reconstructed in the same trigger event, a track is obtained as the line linking the barycenters of the two points. Figure 4 shows the trigger rate and the track flux trends, as functions of the integrated acquisition time, divided in intervals of about 6 h. The muon rate is reduced with respect to the trigger rate to a mean of 8.2 Hz, mostly due to the tighter tracking requirements. Measured muon flux fluctuates within the 2%, improving the oscillations of the trigger rate, proving the robustness of the tracking algorithm.

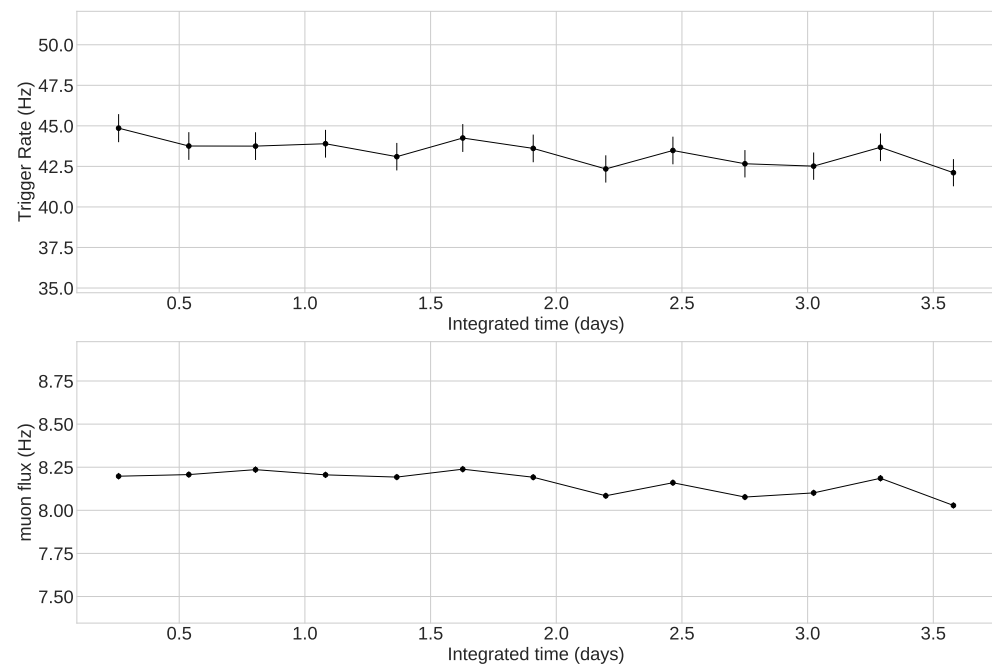


Figure 4. (Top): trigger rate trend, measured in free-sky mode acquisition with the detector installed vertically. (Bottom): muon rate, obtained from free-sky data by applying the tracking algorithm.

In order to compare the measured muon flux with expectations, a Monte Carlo simulation has been developed to verify the detector capabilities. The simulation provides a simple numerical evaluation of the geometrical acceptance and the muon flux is analytically calculated by integrating Gaisser’s modified formula [6]. The results are reported as bidimensional map in $\theta - \phi$ muon direction coordinates and shown in Figure 5; the color scale represents the muon rate in Hz.

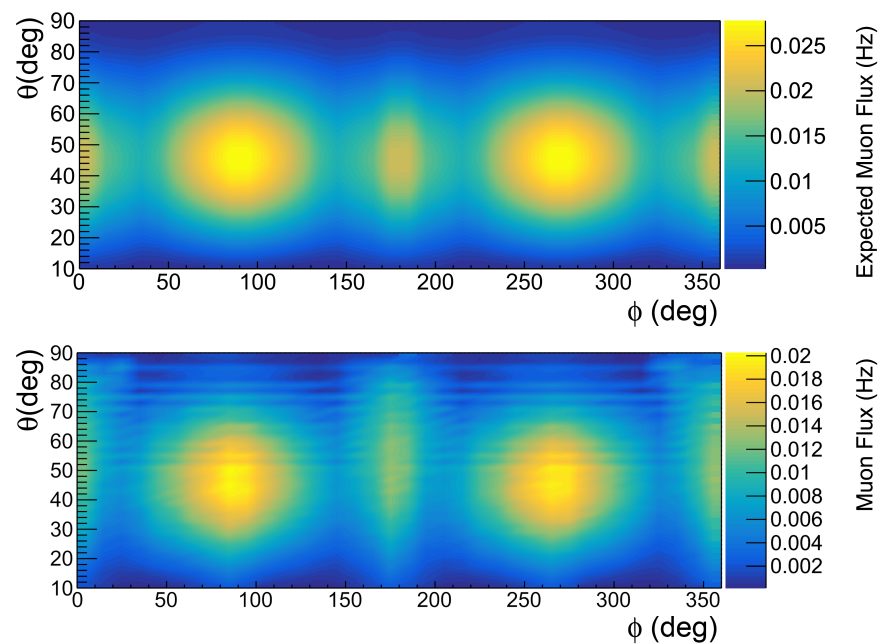


Figure 5. Expected (**top**) and Observed (**bottom**) muon rates in free-sky exposure and vertical orientation. The comparison between observed and expected fluxes results in a good agreement.

4. Validation On-Site

The detector was specifically built to fit into wells and to maximize efficiency under such conditions. However, it was decided to preliminarily test and study the detector's performance in a known environment, where the detector's ability to detect empty chambers in the overlying rock could be easily proven, even though it is not a borehole. The underground of the Mt. Echia, a hill in the core of the city of Naples (Italy), has been chosen as validation field. The site was partially probed with a planar muon detector in the past [7,8], reaching impressive results. Since large planar detectors, even being portable, are more difficult to move around, the previous experience with the MU-RAY apparatus only investigated two locations. The compactness and peculiar portability of the new cylindrical muon detector allows for easily relocation, useful in the case a three-dimensional image would be provided.

Mt. Echia is made of Neapolitan yellow tuff and hosts in its underground the so-called Galleria Borbonica (Bourbon tunnel), a tunnel linking the King's palace to an escape exit on the opposite side of the city, built by order of king Ferdinando II of the Bourbon house. Furthermore, a complex and even more ancient system of galleries and chambers have been excavated and are partially available to the public. In this scenario, the detector was moved in different installation points, chosen around a known cavity, aiming to provide sufficient data to investigate possible improvement of the 3D reconstruction algorithm described in [8].

A first observation has been promptly seen: the underground trigger rates were higher than in free-sky exposition. In Figure 6 two examples of trigger rate acquired in different underground locations are reported. The measured trigger rates are on average 90 and 77 Hz, while in the free-sky the mean trigger rate was almost half these values. Applying the tracking algorithm, the measured muon rates decrease to the level of about 0.69 and 0.64 Hz (Figure 7), that are acceptable according to the expected rock absorption degree.

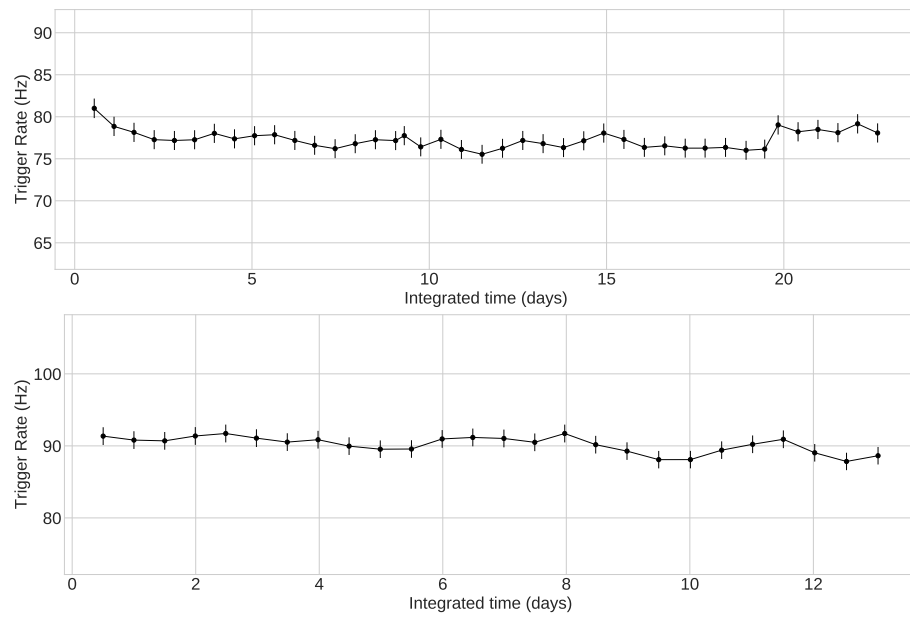


Figure 6. Trigger rate trends in two different locations of the Mt. Echia underground. In particular, the top plot refers to a position in one chamber that is located deeper underground with respect to the Galleria Borbonica, and the bottom plot refers to a position inside the GB.

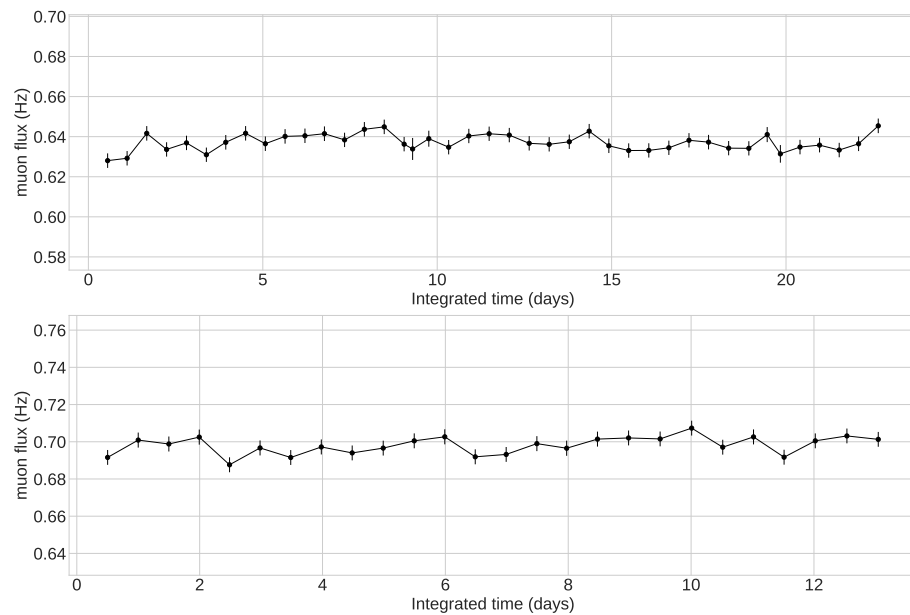


Figure 7. Track rate trends in two different locations of the Mt. Echia underground. In particular, the top plot refers to a position in one chamber that is located deeper underground with respect to the Galleria Borbonica, and the bottom plot refers to a position inside the GB. These fluxes are obtained from fluxes in Figure 6 by asking for the presence of two muon crossing points, which is the minimum requirement to get a track.

Investigating the origin of this over-triggering of the detector, we concluded that the most reasonable source activating the detector is environmental radioactivity, as is expected from simulations described in [9]. As can be found in literature [10], the volcanic yellow tuff contains many radioactive isotopes, as ^{232}Th , ^{226}Ra and ^{40}K . The decay chains of these elements led to production of α , β and γ particles. Since the detector shell provides adequate shielding against alpha and beta particles, we are quite confident that the source of these signals are gammas. For instance ^{232}Th daughters ^{212}Bi , ^{208}Tl and ^{228}Ac

produce gammas of 727, 860 and 911 keV respectively, energies high enough to fulfill the trigger requirement.

Even through the spurious signals are mostly removed applying the tracking algorithm, a small fraction of remaining contamination is spotted out in the track energy distributions. Indeed, as can be seen in Figure 8, a second smaller peak is observed in addition to the principal one, related to muons. A countercheck of the falseness of these tracks is that this lower energy peak is not present in the energy distribution of the free-sky reconstructed tracks (Figure 9).

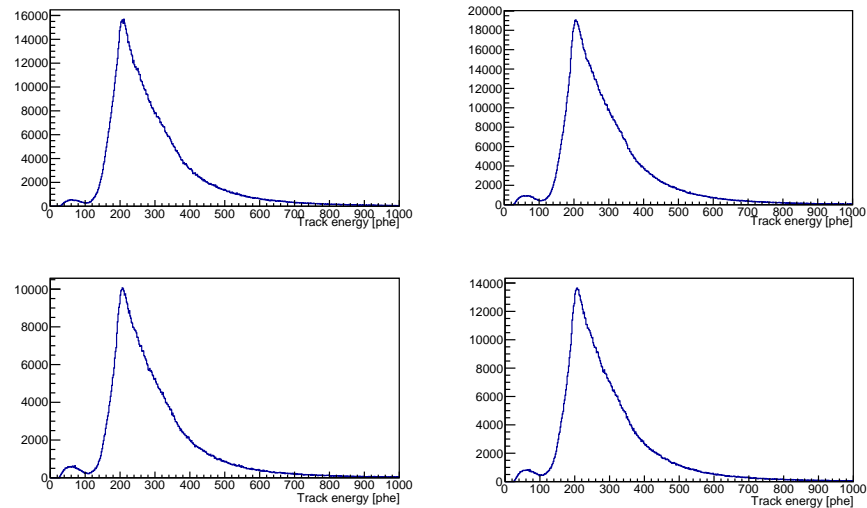


Figure 8. Track energy distributions of four different datasets, taken from different locations. Each distribution presents a small peak at energies just below 100 photoelectrons. These events are considered as spurious tracks related to one or more hit generated by radioactivity of the rock. Therefore a cut for energies above 100 photoelectrons has been applied.

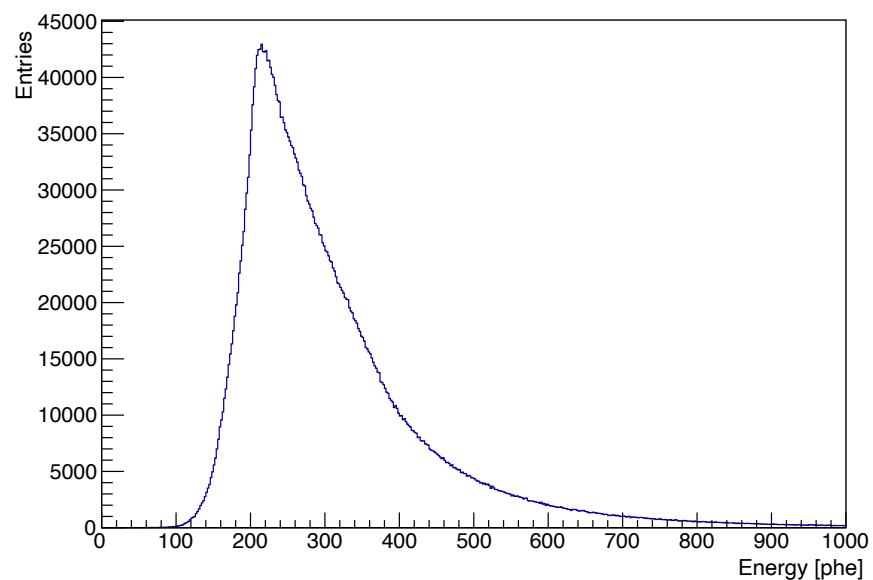


Figure 9. Track energy distribution resulting from free sky data acquisition.

Then, to reduce this background contamination to a level as low as possible we decided to apply an energy cut on the track energy in between the two observed peaks.

The stability of the measured muon flux and the lower level of fluctuations with respect to the trigger rate can be taken as a first meaningful demonstration of good performance

of the detector and associated reconstruction algorithms. The underground muon rates shown in Figure 7, present maximum variations around the mean values under the level of 3%, almost halving the trigger rate fluctuations. All the datasets, taken in several different locations present similar behaviors. The capability of the borehole cylindrical detector to provide clear evidence of the presence of cavities in the inspected volumes has been proved by results of this first test on-field. In particular the first location where the detector has been installed corresponds to the already adopted location in the context of the MU-RAY experiment. A muon radiography study has been performed with an amount of data corresponding to about one week and the resulting image has been compared with what was already obtained with MU-RAY data. After accounting for slight differences in the positioning of the two detectors and polar inefficiencies of the borehole detector due to the PD angular gaps, identical structures appear to be identified by the bore-hole detector and the MU-RAY detector (Figure 10). The evidence of corresponding signals, indicated as A, B and C, proves that performance of the new cylindrical detector in this scenario is compatible with ones of a planar 1 m² detector, even if the two compared images result from different amounts of data, that are about 5 and 20 days of data taking respectively for the cylinder and MU-RAY. Signals indicated in Figure 10 have been also identified, by simulations, as known cavities. In particular the B and C correspond to the chambers chosen as test in [7], while signal A corresponds to another known chamber, referred to as the “dome”.

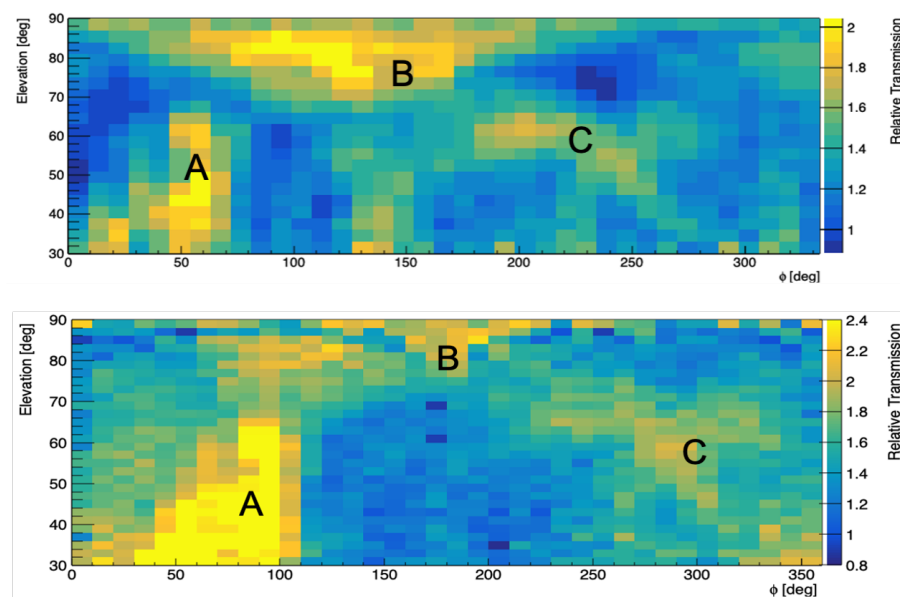


Figure 10. MU-RAY (**top**) and cylinder (**bottom**) relative transmission maps obtained from the same location in the Mt. Echia underground.

Conclusions

Muon radiography is rapidly developing as an alternative and non-invasive tool to investigate the presence of cavities below large buildings or hills. One major difficulty of muon radiography in this application is related to the necessity of installing a muon detector deeper than the volumes to be inspected, meaning that an underground available and easily accessible space is required, and also a power supply system is needed to feed the apparatus.

In this paper, we describe a new compact, portable and low power consuming muon detector, recently developed for muon radiography application. The new borehole cylindrical detector has been particularly designed to be inserted in drilled wells, overcoming the problem of the installation point.

The sensitive surface of the detector has a cylindrical shape, realized by using arc-scintillators maximizing the acceptance of this geometry.

Tests have been conducted both exposing the detector to free sky muon flux and measuring underground muon transmission through tens of meters of rock. Good performance and stability were observed in both exposures. The capability of detecting the presence of cavities hidden in the rock has been validated in a preliminary field application.

Author Contributions: Conceptualization, G.S. and L.C.; methodology, M.D.; software, M.D. and L.C.; validation, L.C., M.M. and F.A.; formal analysis, M.D.; investigation, G.S.; resources, L.R. and V.M.; data curation, M.D.; writing—original draft preparation, M.D.; writing—review and editing, G.S.; visualization, M.D.; supervision, F.A.; project administration, G.S. and F.A.; funding acquisition, G.S. and F.A. All authors have read and agreed to the published version of the manuscript.

Funding: This research was funded by the Italian Ministry for Education, University and Research (PON R&C 2007-2013, DD 713Ric of the 29 October 2010 Tit III) in the frame of the project METROPOLIS—PON 03PE 00093 4 (DD MIUR prot. no. 0000791 of the 6 March 2014), supported by STRESS Scarl company.

Data Availability Statement: Not applicable.

Acknowledgments: Authors warmly thank the technical staff of the INFN of Naples for their support in electronics development, the mechanical design and the detector assembly. The authors gratefully acknowledge the support of G. Minin and the other members of the Galleria Borbonica association. Finally the authors express their gratitude to D. Sala, and L. Amato (TECNO-IN S.P.A.), M. Esposito and V. James (STRESS S.c.a r.l.).

Conflicts of Interest: The authors declare no conflict of interest.

References

1. Vanini, S.; Ambrosino, F.; Bonechi, L.; Bonomi, G.; Checchia, P.; D'Alessandro, R.; Nebbia, G.; Saracino, G.; Zenoni, A.; Zumerl, G. Cultural heritage investigations using cosmic muons. *Comptes Rendus Phys.* **2018**, *19*, 533–542. [\[CrossRef\]](#)
2. D'Errico, M. Muography applied to Archaeology: Search and 3D reconstruction of hidden cavities. *IL Nuovo C* **2020**, *43*, 126. [\[CrossRef\]](#)
3. Morishima, K.; Kuno, M.; Nishio, A.; Kitagawa, N.; Manabe, Y.; Moto, M.; Takasaki, F.; Fujii, H.; Satoh, K.; Kodama, H.; et al. Discovery of a big void in Khufu's Pyramid by observation of cosmic-ray muons. *Nature* **2017**, *552*, 386–390. [\[CrossRef\]](#) [\[PubMed\]](#)
4. Cimmino, L.; Ambrosino, F.; Bonechi, L.; Ciaranfi, R.; D'Alessandro, R.; Masone, V.; Mori, N.; Noli, P.; Saracino, G.; Strolin, P. The MURAVES telescope front-end electronics and data acquisition. *Ann. Geophys.* **2017**, *60*, 1. [\[CrossRef\]](#)
5. Fleury, J. EASIROC, an Easy and Versatile ReadOut Device for SiPM. *Phys. Procedia* **2012**, *37*, 1569.
6. Gaisser, T.K.; Engel, R.; Resconi, E. *Cosmic Rays and Particle Physics*; Cambridge University Press: Cambridge, UK, 2001.
7. Saracino, G.; Amato, L.; Ambrosino, F.; Antonucci, G.; Bonechi, L.; Cimmino, L.; Consiglio, L.; D'Alessandro, R.; De Luzio, E.; Minin, G.; et al. Imaging of underground cavities with cosmic-ray muons from observations at Mt. Echia (Naples). *Sci. Rep.* **2017**, *7*, 1038. [\[CrossRef\]](#) [\[PubMed\]](#)
8. Cimmino, L.; Baccani, G.; Noli, P.; Amato, L.; Ambrosino, F.; Bonechi, L.; Bongi, M.; Ciulli, V.; D'Alessandro, R.; D'Errico, M.; et al. 3D Muography for the Search of Hidden Cavities. *Sci. Rep.* **2019**, *9*, 2974. [\[CrossRef\]](#) [\[PubMed\]](#)
9. Flygare, J.; Bonneville, A.; Kouzes, R.; Yamaoka, J.; Lintereur, A. Muon Borehole Detector Design for Use in 4D Density Overburden Monitoring. *IEEE Trans. Nucl. Sci.* **2017**, *65*, 2724–2731. [\[CrossRef\]](#)
10. Roca, V.; Sabbarese, C.; D'Onofrio, A.; Lubritto, C.; Terrasi, F.; Ermice, A.; Inghima, I.; Migliore, G. Natural radioactivity of building materials coming from a volcanic region. In Proceedings of the 4th European Conference on Protection against Radon at Home and at Work, Prague, Czech Republic, 28 June–2 July 2004.

Disclaimer/Publisher's Note: The statements, opinions and data contained in all publications are solely those of the individual author(s) and contributor(s) and not of MDPI and/or the editor(s). MDPI and/or the editor(s) disclaim responsibility for any injury to people or property resulting from any ideas, methods, instructions or products referred to in the content.